Adsorbed states and the kinetics of electrooxidation of phenols on metal oxides

Carlos Borras*, Jorge Mostany and Benjamín R. Scharifker

Departamento de Química, Universidad Simón Bolívar, Apartado 89000,
Caracas 1080A, Venezuela.

Abstract

We discuss the role of adsorbed states in determining the kinetics of electrochemical oxidation of substituted phenols on various metal oxide surfaces. On antimony-doped tin oxide (SnO_2-Sb) electrodes, oxidation of both p-methoxyphenol (PMP) and p-nitrophenol (PNP) follow Langmuir-Hinshelwood kinetics: at high concentrations of phenol in solution, the oxidation rates are controlled by surface processes. In general, anodic oxidation of PMP and PNP on SnO_2-Sb electrodes leads to complete mineralization to CO_2. Under surface saturation conditions, however, oxidation of PNP occurs to a lower extent due to the encumbered formation of OH surface species required for complete oxidation. The role of adsorbed states is further illustrated examining the effects of competing adsorption of p-chlorophenol (PCP) and PNP on bismuth-doped lead oxide (PbO_2-Bi) electrodes. It is shown that due to stronger adsorption, the presence of PNP inhibits the oxidation of PCP.

Key words: Electrocatalysis; metal oxide anode; oxidation of organic compomds; p-methoxyphenol; p-nitrophenol.

Estados adsorbidos y la cinética de la electro-oxidación de fenoles sobre óxidos metálicos

Resumen

Se discute el papel de los estados adsorbidos en la cinética de oxidación electroquímica de fenoles substituidos en superficies de óxidos metálicos diversos. Sobre electrodos de óxido de estaño dopado con antimonio (SnO_2-Sb), la oxidación tanto de p-metoxifenol (PMP) and p-nitrofenol (PNP) sigue una cinética de Langmuir-Hinshelwood; a altas concentraciones de fenol en solución, los estados de oxidación están controlados por procesos superficiales. En general, la oxidación anódica de PMP y PNP sobre electrodos de SnO_2-Sb lleva a la mineralización total a CO_2. Sin embargo, en condiciones de saturación superficial la oxidación de PNP ocurre en un menor grado debido a la adsorción mayoritaria de radicales OH en la superficie, que son requeridos para una oxidación completa. Adicionalmente, el papel de los estados adsorbidos se ilustra examinando los efectos de la adsorción competitiva de p-clorofenol (PCP) y PNP en electrodos de óxido de plomo dopado con bismuto (PbO_2-Bi). Se muestra que debido a una mayor adsorción del orgánico, la presencia de PNP inhibe la oxidación de PCP.

Palabras clave: Ánodo de oxido metálico; electrocatálisis; oxidación de organismo; p-metoxifenol; p-nitrofenol.

*   Autor para la correspondencia. E-mail: cborras@usb.ve

Introduction

Expansion of human development in a still growing world population requires industrial outputs at increased rates, imposing further demands on the environment. The environmental impact of industrial processes often limits the possibilities for sustainable growth, hence the current concern on the development and implementation of efficient methods for the removal of pollutant waste and by-products.

The electrochemical oxidation of phenols involves OH_{ads} radicals on the surface of the anode, formed from decomposition of water. This mechanism was postulated in 1985 (1-7) and is now widely accepted. Oxidation is preceded by transport of the reactant in solution (R_{sol}) towards the electrode surface, followed by adsorption on catalytic sites at the metal oxide anode, $Mo_x[ ]$ (8).

$$R_{sol} \rightarrow R_{elec} \qquad [1]$$

$$R_{elec} + MO_x[] \rightarrow MO_x[R] \qquad [2]$$

Adsorbed hydroxyl radicals also form at the metal oxide surface from reaction with water, with electron transfer and generation of protons,

$$MO_x[ ] + H_2O \rightarrow MO_x[OH\cdot] + H^+ + e^- \qquad [3]$$
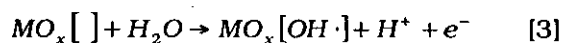
and transfer of oxygen atoms to the organic molecule results from reaction of the adsorbed species with regeneration of adsorption sites on the surface:

$$MO_x[OH\cdot] + MO_x[R] \rightarrow 2MO_x[ ] + ROH \qquad [4]$$
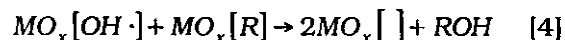
Oxygen evolution is an undesired but unavoidable parallel reaction under these conditions, occurring from the recombination of adsorbed hydroxyl radicals,

$$2MO_x[OH\cdot] \rightarrow 2MO_x[ ] + O_2 + 2H^+ + 2e^- \qquad [5]$$
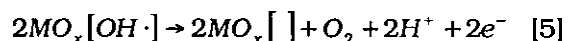
In principle any organic compound might be oxidized on conducting surfaces at electrode potentials positive enough to form hydroxyl radicals. Notwithstanding, oxidation of phenols on noble metal anodes such as Pt or Au, even though adsorbed hydroxyl radicals are readily formed, leads to swift passivation of the electrode and very low oxidation rates due to formation of an impervious film on the surface from the electropolymerization of phenol (9-13). The first step of the anodic reaction is formation of the phenoxy radical with the loss of an electron. This may react with another phenoxy radical with subsequent polymerization, or oxidize with oxygen transfer from an OH radical to yield quinones compound, aliphatic acids and CO_2.

The extent of the reaction is chiefly governed by the catalyst species facilitating oxygen transfer to the organic compound. The prevailing model proposed for this kind of reactions involves adsorption of the organic compound on the catalyst surface, followed by electron transfer and reaction on the electrode with OH radicals present on the surface, produced from discharge of water (14). It has been found that some phenols adsorb on various surfaces following the Langmuir isotherm (15-18), and that the effects of changes of temperature on the reaction rate are determined by the adsorption and desorption equilibria of the species involved at the respective temperatures. Competitive effects arise in solutions with more than one phenolic compound present (19, 20), as it is frequently the case in dealing with waste waters. These impinge on the coverages of the various compounds on the electrode surface and hence affect their rates of oxidation.

Here we discuss the importance of adsorbed states on the kinetics of oxidation of several substituted phenols on various surfaces. Results obtained using Uv-vis spectrophotometry and HPLC analyses indicate different reaction mechanisms, determined by the nature of initial adsorption of the starting compound on the electrode surface. At increasing concentrations of the phenols

in solution the oxidation rate becomes limited by reaction of the adsorbed species with surface OH generated from water decomposition on the metal oxide, following Langmuir-Hinshelwood kinetics. We also analyze and discuss competitive effects arising in the joint presence of more than one phenol in solution, affecting the rate of their oxidation on the metal oxide surfaces.

Experimental

Working electrodes were prepared from antimony-doped tin oxide thin films deposited on glass substrate, with sheet resistance of ~70 Ω/square, obtained from PPG industries, Inc. Electrical contacts to silver wires were realized with silver-loaded epoxy, and these assemblies were isolated with Teflon® thermally shrinkable tubing in order to expose ca. 1 cm^2 of Sb-SnO$_2$ surface to the solution. Measurements were conducted using a three-compartment glass cell, maintaining the solution in the working electrode compartment separated from that contacting the 2.2 cm^2 platinum wire used as secondary electrode with a glass frit. A saturated calomel electrode (SCE) was used as reference, and all potentials are reported with respect to the SCE unless otherwise stated. Reagents were of analytical grade (Aldrich or Sigma) and all solutions were prepared with distilled and ultrafiltered (Nanopure®) water.

Electrolysis at constant potentials were carried out with an EG&G PAR model 273 potentiostat, using working electrodes as described above and platinum gauze with larger geometrical surface area as counter electrode. The working electrode compartment was filled for these experiments with 20 mL of phenol-containing solution. The charge at any time of electrolysis was determined from integral of cronoamperogram.

The variation of PNP concentration during electrolysis at constant potential was determined from UV-Vis spectra. Spectroscopic data were obtained with a Hewlett-Packard 8452A diode-array spectrometer

under HP 89531 MS-DOS UV/Vis Operating Software, from 100 l aliquots sampled from the electrolysis cell at different times, and diluted to 10 mL with water. The experimental UV-Vis spectra thus obtained were deconvoluted into Lorentzian bands with Jandel Peakfit v. 3.0. PNP concentrations in solution were determined using the Lambert-Beer law, with molar absorption coefficient ε= 9.1 10^3 cm^1 M^1 obtained from calibration curve data at the wavelength of maximum absorption.

Liquid chromatography was carried out with a Water Association HPLC system composed of a Model M6000A pump, a Ryhodine injector, a Model 484 UV detector and a Model 745B data recorder. A Nova-Pack C18, 3.9×150 mm column was used to determine phenol and quinones, with 60/40 methanol/water solution as mobile phase, at 0.8 mL/min flow rate and 254 nm UV-vis detection. Aliphatic acids were analyzed with an Aminex HPX-87, 7.8×300 mm column, using 8×10^4 M sulfuric acid aqueous solution as mobile phase at 0.5 mL/min flow rate, with detection at 210 nm.

In situ infrared spectra of the Bi-PbO$_2$|solution interface during electrolysis were acquired with a Bruker Equinox IFS-55 spectrometer, with a medium band (MIR, 700-6000 cm^1) globar source and liquid nitrogen-cooled MCT detector, on a mirror-polished Bi-PbO$_2$ film deposited onto a flat 1 cm diameter Au disc, set against a CaF$_2$ window to form a thin layer cell. Each spectrum was obtained by Fourier transformation after averaging 150 interferograms during 75 s at 8 cm^1 resolution, using p-polarized radiation, at constant potential of 1.65 V vs SCE.

Results and Discussion

Figure 1 shows deconvoluted UV-Vis spectra of 10^3 M PMP (Figure 1a) and 10^3 M PNP (Figure 1b) solutions in aqueous 0.1 M Na$_2$SO$_4$, after 30 minutes electrolysis at 2.5 V vs SCE. In Figure 1a, the bands between
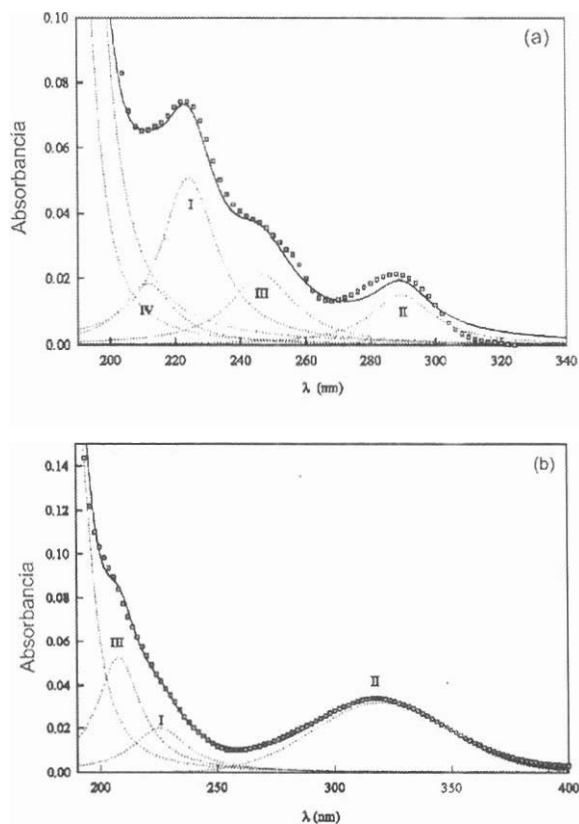
Figure 1. Spectra obtained during oxidation of p-methoxyphenol (a) and p-nitrophenol (b). Intensities of experimental (□) and deconvoluted (—) absorption bands.

210-240 nm (I) and 265-310 nm (II) are associated to the starting compound. The band between 230-265 nm (III) increases as PMP is oxidized. This band arises from the oxidation of phenol to a quinoid compound, turning the solution yellow due to the increased conjugation of double-bonds in the molecule. This has been reported as the principal reaction intermediate during oxidation of several phenolic compounds (1, 21), a result that was verified with high performance liquid chromatography (HPLC) confirming, from analysis of aromatics, that benzoquinone (BQ) was the principal product. Formation of BQ suggests that metha-

nol is also formed as secondary product. The band centered at 210 nm (IV) appears after the passage of larger charges through the electrode|solution interface, and corresponds to aliphatic acids (AA) formed from oxidation with rupture of the aromatic ring. HPLC analysis of samples taken from 10^3 M PMP + 0.1 M Na_2SO_4 solution after electrolysis at 2.5 V corroborates that maleic acid was the principal AA. Figure 1b shows the UV-Vis spectrum of 10^3 M PNP and 0.1 M Na_2SO_4 aqueous solution after 30 minutes of electrolysis. The bands located between 210 and 250 nm (I), and between 260 and 370 nm (II), are attributed to the reacting species and decrease as oxidation proceeds. In contrast to the result shown above related to the oxidation of PMP, the HPLC response of samples obtained after passing 70 C dm^3 in 10^3 M PNP + 0.1 M Na_2SO_4 solutions show that the band centered at 210 nm (III) corresponds to the presence of nitrite ions in solution, produced by the release of the nitro group from the PNP molecule, and very low concentration of aliphatic acids. The absence of a band at 250 nm indicates that BQ (or any other quinoid compound) does not accumulate in solution.

The following scheme of consecutive reactions describes the results obtained, oxidation of PMP occurs through mechanism 1, with BQ and AA having been identified as the principal electrolysis products appearing in solution. Even though hydroquinone is the first product formed according to this mechanism, it has not been identified in solution because its oxidation by direct transfer of two electrons occurs instantaneously (8). Oxidation of PNP, on the other hand, may be represented by mechanism 2, with AA formed from the onset of electrolysis. Both compounds react on the same electrode surface; however their oxidation mechanism is different indicating different surface orientations of the adsorbed molecule.

Mechanism 1
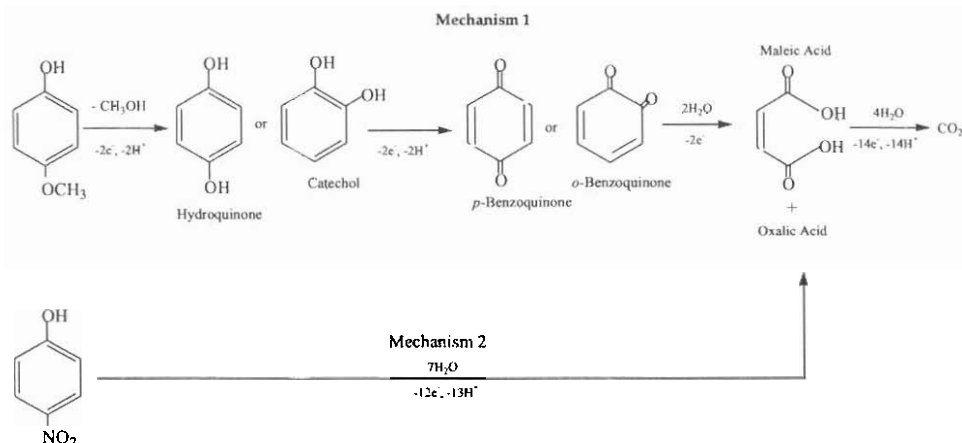
Mechanism 2

Concentration effects

Figure 2 shows the initial oxidation rate of PMP and PNP as a function of their respective initial concentration in solution. The kinetics is well represented by the Langmuir-Hinshelwood mechanism (22-55), according to which at high phenols concentrations the oxidation rate becomes lower than the adsorption rate, and the kinetics becomes limited by the availability of adsorption sites on the electrode surface.

At oxidation rates much lower than the adsorption rate, the overall rate equation may be written as

$$r = k N_0\, \theta_{OH} \theta_{ph} \qquad [6]$$

where k is the oxidation rate constant, N_0 represents the surface density of adsorption sites (cm^2), θ_{ph} is the fractional surface coverage by phenol and θ_{OH} is the coverage of the surface by OH$_{ads}$ arising from the discharge of water. θ_{OH} cannot be expressed in terms of a Langmuir isotherm since does not correspond to an adsorption-desorption equilibrium. However we may consider that its value remains constant at a given interfacial potential, thus for constant potential we may write that

$$k_{app} = k N_0\, \theta_{OH} \qquad [7]$$
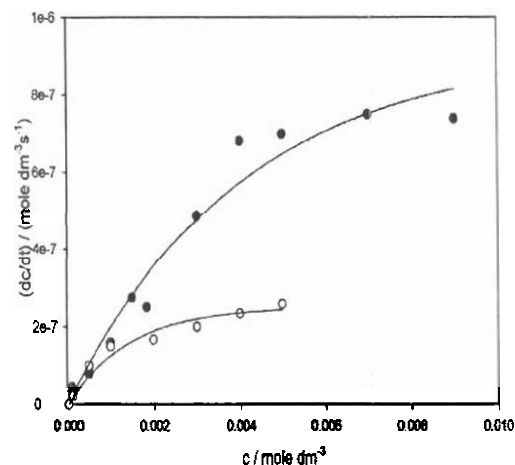
Figure 2. Initial oxidation rate of p-methoxy-phenol (●) and p-nitrophenol (O) as a function of their initial concentration in solution.

θ_{Ph}, the fraction of adsorption sites on the surface occupied by adsorbed Phenol (PMP or PNP), under Langmuir conditions may be represented as:

$$\theta_{Ph} = K_{Ph}\, c_{Ph} \,/\left(1 + K_{Ph} c_{Ph}\right) \qquad [8]$$

where K_{Ph} is the adsorption/desorption equilibrium constant. According to [8] at high Ph concentration $K_{Ph} c_{Ph} \gg 1$ and $\theta \approx 1$, i.e., the surface is almost totally covered

with Ph. Consequently, at sufficiently high concentration,

$$r = k_{app} \tag{9}$$

and the reaction is zeroth order with respect to the Ph solution concentration; under such conditions the reaction rate becomes independent of the concentration of Ph.

This result confirms that the observed behavior in the mineralization mechanism of PMP and PNP originates from the different interactions established between these compounds and the oxide surface, probably due to the distinct electronic characters of the respective substituting groups.

Taking into account that the degradation reaction follows first order kinetics, the kinetic constant may be obtained from:

$$dc_{Ph} / dt = k_{app} c_{Ph} \tag{10}$$

The integral form of |9] is:

$$-\ln c_{Ph/c_{Ph,0}} = k_{app} t \tag{11}$$

where $c_{Ph,0}$ is the initial concentration of phenol. From the slopes of linear plots of ln $c_{Ph}/c_{Ph,0}$ vs t, values for k_{app} can be obtained. From this kinetic analysis it follows that $k_{app} = 5 \times 10^5$ s^{-1} in the whole range of PMP concentrations studied. However the k_{app} values determined for oxidation of PNP showed dependence on the initial solution concentration of PNP, as shown in Figure 3.

From the values in the Figure 3 it may be observed that the apparent rate constant *decreases* with the *increase* of the initial PNP concentration, up to a value corresponding to saturation of PNP at the surface, above which k_{app} remains constant. Considering that $k_{app} = k N_0 \theta_{OH}$, then the drop of k_{app} may be attributed to the diminution of one or more of the three factors k, N_0 or θ_{OH}. Since a fresh electrode was used for each experiment in order to avoid effects due to passivation, blocking or fouling of the surface, we may infer that the density of adsorption sites
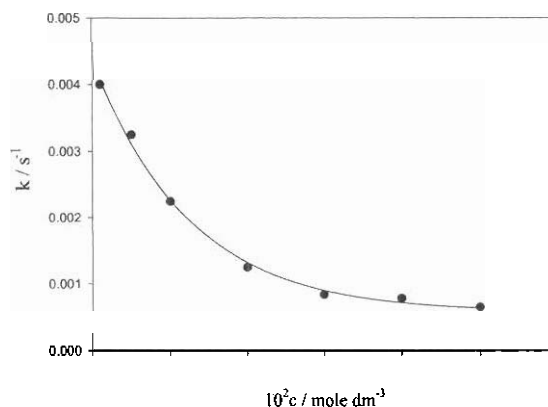
Figure 3. Oxidation rate constant as a function of the p-nitrophenol initial concentration in solution.

N_0 remained unchanged throughout the experiments. The result is therefore associated to the decreased OH surface concentration due to occupation of surface sites by adsorbed PNP, or else by the unavailability of surface sites for adsorption of the generated intermediates.

The results obtained from spectrophotometric measurements were contrasted with those obtained using electrochemical techniques. Figure 4 shows the electric charge Q circulated across the cell as a function of the PNP concentration.

From to the Faraday equation,

$$Q = nFcV \tag{12}$$

where nF is the molar oxidation charge and V is the volume of electrolyzed solution. Then from the slope dQ/dc at known V the number of electrons transferred n may be obtained. Figure 5 shows the values of n obtained according to [11] as a function of the initial PNP concentration in solution.

Two distinct regimes are observed. Electrolysis at $c_{PMP} \leq 0.002$ M involves $n \approx 20$, indicating the nearly complete oxidation of the starting compound leading to mineralization to CO_2, whereas at higher concentrations the number of electrons transferred
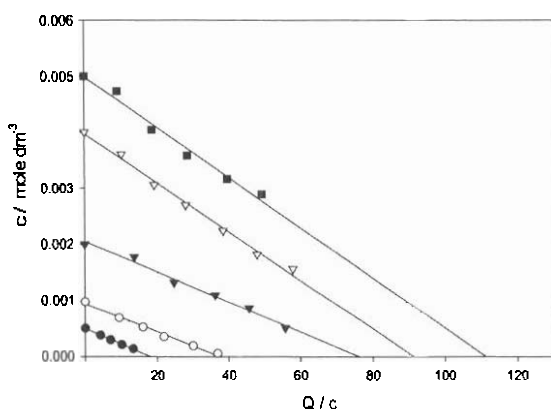
Figure 4. Electric charge Q transferred across the electrode-solution interface, as a function of the p-nitrophenol concentration.
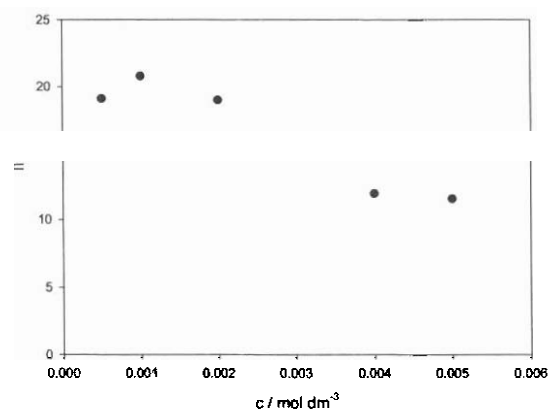
Figure 5. Number of moles of electrons transferred per mol of p-nitrophenol oxidized, as a function of the p-nitrophenol concentration.

per mole of oxidized PNP is somewhat lower, $n \approx 12$, leading to the accumulation of aliphatic acids which were indeed detected in solution. Thus the mechanism of electrooxidation of phenols in general depends on the surface coverage, and at high coverage on $Sb-SnO_2$ total mineralization of PNP to CO_2 is impeded.

Competitive adsorption of PCP and PNP on Bi-PbO$_2$

Adsorption of PCP and PNP on $Bi-PbO_2$ was studied at open circuit. The changes in concentration following immersion of large-area $Bi-PbO_2$ electrodes in aqueous solutions of the phenols were determined from UV-Vis spectra of the solutions obtained at different times. The PCP concentration first diminishes and then approaches a steady value corresponding to the establishment of adsorption equilibrium at the electrode | solution interface. The adsorption rate was not affected by solution stirring at different rates, thus under the present conditions diffusion of PCP towards the electrode surface is not rate-limiting.

As shown in Figure 6 adsorption is well described with the Langmuir model under all conditions studied. This result shows that the kinetics of PCP adsorption may depend on the availability of free adsorption sites on the surface of the catalyst.

Figure 7 shows that the presence of PNP affects the rate of adsorption of PCP. The rate of PCP adsorption decreases as the concentration of PNP in solution is increased, due to competition of both species for adsorption sites on the surface. At sufficiently high PNP concentrations, 3×10^5 M PNP in this case, the rate of PCP adsorption did not diminish with increasing concentrations of PNP, thus indicating the preferred adsorption of PNP molecules on the active sites on the surface.

Considering further that the surface concentration of the species involved controls their oxidation rate, then the respective oxidation yields, in the presence of several phenolic compounds in solution, depend on the relative strengths of their interactions with the surface. Thus we electrolyzed a solution containing equal initial concentrations $(10^3$ M) of PCP and PNP, and followed the concentration decay of these compounds as a function of the electric charge passed.
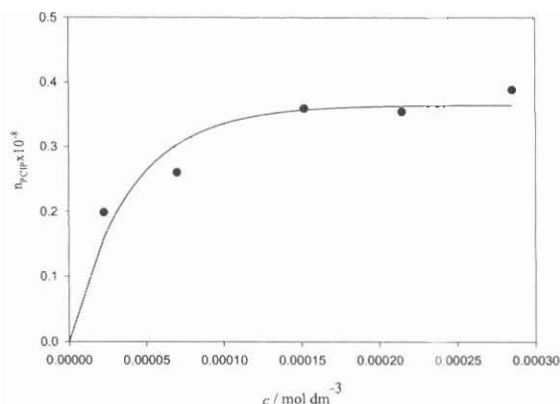
Figure 6.   Number of moles of p-chlorophenol adsorbed on the electrode surface as a function of the equilibrium concentration of p-chlorophenol in solution.
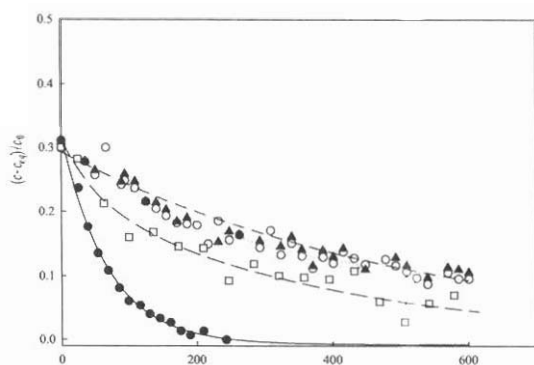
Figure 7.   Decay of the normalized p-chlorophenol concentration in the absence of p-nitrophenol in solution (●), and in the presence of 2×10^5 M (■), 3×10^5 M (▲) pnp and 5×10^5 M (□). c_{eq} is the equilibrium concentration of p-chlorophenol in solution after adsorption in the absence of p-nitrophenol.

Figure 8 shows the concentration decay of PCP during electrolysis of a solution without PNP, or in the presence of both in equimolar concentrations, as a function of the electric charge passed. The coulombic yield
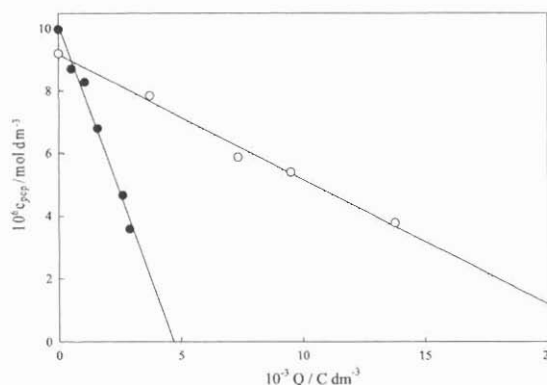
Figure 8.   p-chlorophenol concentration as a function of electric charge passed during electrolysis at 1.65 V vs SCE in 0.001 M p-chlorophenol + 0.1 M Na_2SO_4 (●), and 0.001 M PCP + 0.001 p-nitrophenol + 0.1 M Na_2SO_4 (O) solutions.

observed was 2.2×10^7 mol C^1 in solution of PCP only, and 0.39×10^7 mol C^1 in equimolar solution of PCP and PNP. As shown above from the adsorption studies, the preferred oxidation of PNP when both PNP and PCP are present in solution is due to stronger adsorption of PNP on the surface.

The very short life-time in solution of the OH radicals produced on the substrate limit the reaction zone to the surface of the catalyst (26). Therefore, the rate of each stage of oxidation depends on the surface concentration of the respective organic compound, in turn depending on their corresponding adsorption equilibrium constants and bulk concentrations. Mineralization to CO_2 requires then that intermediates either remain adsorbed on the electrode surface or attain sufficient bulk concentration. Hence, the amounts of produced intermediates, as well as the rate of each of the consecutive steps of the reaction, are strongly dependent on the interactions of the starting compounds with the electrode surface. As we showed above, PCP adsorption on $Bi-PbO_2$ surfaces is affected by the presence of PNP

in solution due to stronger adsorption of PNP (27).

The reliability of vibrational spectroscopy in the characterization of adsorbed substances on conducting electrodes has been demostrated by other authors (28, 29). Figure 9 shows SNIFTIRS spectra of Bi-PbO$_2$ electrodes during PCP and PNP electrolysis at a constant potential of 1.65 V vs SCE. The spectra corresponding to PCP oxidation (Figure 9a) show the appearance of a band at 2342 cm^1, attributed to CO$_2$ produced from oxidation of the organic compound, which grows with electrolysis time. The spectra also show a bipolar band between 1600 and 1800 cm^1 due to the scissor mode vibration of water. No other signals corresponding to the starting species or intermediates were identified; this may indicate weak adsorption of PCP or may be due to surface selection rules related to flat orientation of the adsorbed PCP molecules on the surface of the electrode.

Figure 9b shows the spectra corresponding to PNP oxidation. The negative band at 1290 cm^1 is associated to the NO$_2$ group of the PNP molecule. A wider positive-going band centered around 1330 cm^1 can also be seen in these spectra. This signal corresponds to the nitrate ion (30) and maintains a constant intensity after the second spectrum, indicating fast degradation of PNP to maleic acid (MA) during the initial stages of the reaction, releasing the nitrite ion into solution, followed by fast oxidation to nitrate. Successive spectra show the growth of the band at 2342 cm^1 associated to CO$_2$ production, due to oxidation of the generated MA.

Mineralization of PCP and PNP during these thin-layer experiments was assessed from integration of the CO$_2$ bands obtained during PCP (Figure 9a) and PNP (Figure 9b) oxidation. Figure 10 shows that the integrated intensities obtained during oxidation of both compounds grew at comparable
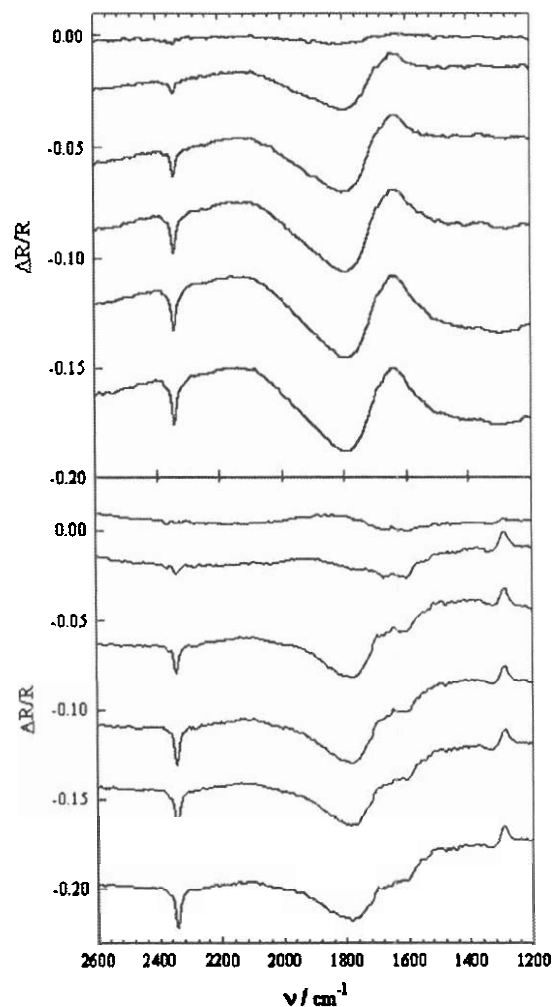
Figure 9. Substractively normalized interfacial FTIR spectra during (a) p-chlorophenol and (b) p-nitrophenol oxidation in aqueous 0.1 M Na2SO4 solution on Bi-PbO2 electrodes. Spectra were acquired at constant potential of 1.65 V vs SCE at 75 s intervals.

rates, confirming complete mineralization in both cases with similar kinetics, and no accumulation of intermediates in solution, under thin layer conditions.
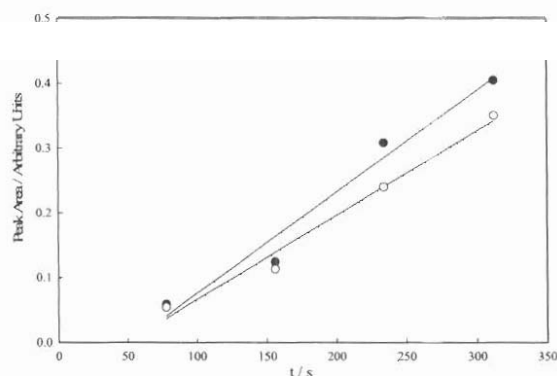
Figure10. Area of CO₂ peaks of Substractively normalized interfacial FTIR spectra obtained during p-chlorophenol (●) and p-nitrophenol (○) electrolysis at 1.65 V vs SCE on Bi-PbO₂, as a function of time.

Conclusion

We have shown that oxidation of phenols substituted with groups of distinct electronic characters (PNP and PMP) on the same electrode surface occurs through different oxidation mechanisms, indicating significant effects due to the initial orientation of the adsorbed molecules on the electrode surface. Increasing the PNP concentration in solution leads to surface saturation, with electrooxidation kinetics following the Langmuir-Hinshelwood model. The oxidation rate constant was found to *decrease* with the PNP concentration in solution, an effect that has been ascribed to restrained coverage of the electrode surface with adsorbed OH as the coverage with adsorbed PNP increases. Furthermore, the oxidation rate of PCP decreases significantly in the presence of PNP, a compound that effectively competes with PCP for oxidation sites on the catalyst surface due to stronger adsorption on the surface of PbO_2-Bi, demonstrating that competitive effects are consequential in the treatment of residual waters and should be considered in studies of the

oxidation of organic compounds on electrode surfaces. Full mineralization to CO_2 requires that intermediates generated during anodic oxidation either remain adsorbed on the electrode surface or attain sufficiently high concentration in solution. Under restrained mass transfer conditions, such as in thin layers, accumulation of intermediates is enhanced, thus in spite of their different interactions with the electrode surface, PCP and PNP show similar mineralization rates, as we have shown with in situ FTIR studies.

Acknowledgements

References

1. COMNINELLIS CH., PULGARIN C. *J Appl Electrochem* 21, 703, 1991.

2. FLESZAR B., PLOSZYNSKA J. *Electrochim Acta* 30, 31, 1985.

3. VITT J.E., JOHNSON D.C. *J Electrochem Soc* 139, 774, 1992.

4. MURPHY O.J., HITCHENS G.D., KABA L., VEROSTKO C.E. *Wat Res* 26, 443, 1992.

5. POPOVIC N.D., JOHNSON D.C. *Anal Chem* 70, 468, 1998.

6. COMNINELLIS CH. *Electrochim Acta* 39, 1857, 1994.

7. MARSELLI B., GARCIA-GOMEZ J., MICHAUD P.A., RODRIGO M.A., COMNINELLIS CH.. *J Electrochem Soc* 150, D79, 2003.

8. TAHAR N. B., SAVALL A. *J Electrochem Soc* 145, 3427, 1998.

9. GATTRELL M., KIRK D.W. *J Electrochem Soc* 139, 2736, 1992

10. GATTRELL M., KIRK D.W. *J Electrochem Soc* 140, 1534, 1993.

11. ROOGERS J.D., JEDRAL W., BUNCE N.J. *Environ Sci Technol* 33, 1453, 1999.

12. JÜTTNER K., GALLA U., SCHMIEDER H. *Electrochim Acta* 45, 2575, 2000.

13. ANDREESCU S., ANDREESCU D., SADIK O.A. *Electrochem Commun* 5, 681, 2003.

14. FLESZAR B., PLOSZYNSKA J. *Electrochim Acta* 30, 31, 1985.

15. MCBRIDE M.B., WESSELINK L.G. *Environ Sci Techno* 22, 703, 1988.

16. GU B., SCHMITT J., CHEN Z., LIANG L., MCCARTHY J.F. *Environ Sci Technol* 28, 38, 1994.

17. BANDARA J., MIELCZARSKI J.A., LOPEZ A., KIWI *Appl Cat B: Environ* 34, 321, 2001.

18. SISMANOGLU T., PURA S. *Colloids and Surfaces A: Physicochemical and Engineering Aspects*. 180, 1, 2001.

19. PENG D., DURAL N.H. *J Chem Eng Data* 43, 283, 1998.

20. AYRANCI E., CONWAY B.E. *J Electroanal Chem* 513, 100, 2001.

21. POLCARO A.M., PALMAS S. *Ind Eng Chem Res* 36, 1791, 1997.

22. HOFFMAN M.R., MARTIN S.T., CHOI W., BAHNEMANN D. *Chem Rev* 95, 69, 1995.

23. MATTHEWS R.W. *J Phys Chem* 91, 3328, 1987.

24. BAXTER R.J., HU P. *J Chem Phys* 116, 4379, 2002.

25. MATTHEWS R.W. *Wat Res* 20, 569, 1986.

26. TURCHI C.S., OLLIS D.F. *J Catal* 122, 178, 1990.

27. BORRAS C., LAREDO T., SCHARIFKER B.R. *Electrochim Acta* 48, 2775, 2003.

28. SHEPPARD N., DE LA CRUZ C. *Catalysis Today* 70 (2001) 3.

29. DE LA CRUZ C., SHEPPARD N. *Spectrochimica Acta Part A: Molecular Spectroscopy* 50, 271, 1994.

30. NAKAMOTO K. Infrared and Raman Spectra of Inorganic and Coordination Compounds, 5th edn., Wiley, N.Y., 1997.